Multibody System Dynamics **11:** 41–61, 2004.

Energy Preserving Time Integration for Constrained Multibody Systems

ELISABET V. LENS[1], ALBERTO CARDONA[1] and MICHEL GÉRADIN[2]
[1]*Centro Internacional de Métodos Computacionales en Ingeniería, CIMEC-INTEC, Conicet-Universidad Nacional del Litoral, Güemes 3450, 3000 Santa Fe, Argentina; E-mail: acardona@intec.unl.edu.ar*
[2]*JRC – IPSC, Ispra, Italy and University of Liège, Belgium; E-mail: michel.geradin@jrc.it*

(Received: 31 December 2002; accepted in revised form: 23 July 2003)

Abstract. This paper describes an energy preserving integration method for the dynamic analysis of nonlinear multibody systems in the presence of nonlinear constraints. The aspects of finite rotation incrementation, discrete energy conservation and the most common constraint types are examined in detail. The application is made to several rigid body examples, including an intermittent contact problem.

Key words: time integration, DAE systems, energy preservation.

1. Introduction

It is a well-known fact that the time integration of the second order, index 3 differential-algebraic equations (DAE) which arise in multibody dynamics may lead to numerical instability when a second order accurate method of Newmark type is used. Nevertheless, the Newmark family of algorithms is unconditionally stable and second-order accurate for the second-order differential equations in the linear regime. The algebraic constraints are the reason for this instability, occurring in the form of increasing oscillations in the acceleration response [9, 11].

This instability can be controlled by introducing a small high frequency dissipation in the algorithm. A wide number of modifications to the Newmark algorithm has been proposed in order to introduce high frequency dissipation preserving the second order accuracy (e.g. the Hilber–Hughes–Taylor scheme [8] and the Hulbert α-generalized method [10]). In this way the stability of the integration of constrained linear systems is ensured.

In the nonlinear regime, stability cannot be verified by the usual methods of analysis based on the study of the transition matrix properties of the scheme. An alternative way to ensure the solution stability is by means of schemes that guarantee the preservation of the total energy of the system.

Simo et al. have introduced energy preserving schemes for unconstrained rigid bodies, nonlineal dynamics of beams and shells and nonlinear elastodynamics

[16]. Similar schemes have been proposed by Betsch and Steinmann for particles systems [4], nonlinear elastodynamics [5], mechanical systems with holonomic constraints [6] and multibody systems with constraints [7]. The schemes proposed by Bauchau for nonlinear flexible multibody systems [1] and nonlinear elastodynamics [3] and the work of Puso [15] for energy-momentum preserving schemes including joints should also be mentioned.

In this work we revisit a scheme originally proposed in [11] by Géradin and Cardona, which is much inspired by Bauchau's work. In this scheme, the equations of motion are discretized in such a way that energy is preserved in the structural part of the system while the constraints are discretized so that their work exactly vanishes. The combination of these two discretization features guarantees the stability of the numerical integration for constrained multibody systems.

The paper is organized as follows: In Section 2 a discrete form of the motion equations is adopted, treating velocities as quasi-coordinates, which allows us to write the kinetic energy in terms of a constant inertia matrix. The time discretization of the equations of motion is done in Section 3, applying the midpoint rule. The concept of *discrete directional derivative* from Gonzalez [12] is used in Section 4 to reformulate the proof of the energy preservation done in [11]. We describe in detail in Section 5 the parameterization of the finite rotations. In Section 6 we analyse the most usual constraints in multibody systems. Finally in Section 7 several numerical simulations of constrained rigid multibody systems are performed, including impact problems.

2. General Formulation of the Dynamics of a Multibody System

Given a conservative mechanical system described in terms of N generalized coordinates $\boldsymbol{q}$ and subjected to R algebraic constraints

$$\boldsymbol{\Phi}(\boldsymbol{q}) = \boldsymbol{0}, \tag{1}$$

its mechanical properties can be derived by an adequate description of its potential energy $\mathcal{V} = \mathcal{V}(\boldsymbol{q})$ and its kinetic energy which can be written without loss of generality in the quadratic form

$$\mathcal{K} = \frac{1}{2}\boldsymbol{v}^T \boldsymbol{M} \boldsymbol{v}. \tag{2}$$

The $(M \times M)$ inertia matrix $\boldsymbol{M}$ can be assumed constant, symmetric and positive definite provided that the velocities $\boldsymbol{v}$ are expressed in a *material frame*. The latter are treated as quasi-coordinates and thus take the form of linear combinations of time derivatives of generalized coordinates

$$\boldsymbol{v} = \boldsymbol{L}(\boldsymbol{q})\dot{\boldsymbol{q}}, \tag{3}$$

being $\boldsymbol{L}(\boldsymbol{q})$ a $(M \times N)$ matrix [17].

The inequality $M \leq N$ covers the case where the angular velocities description is made in terms of redundant rotation parameters such as the Euler parameters. In this case the redundancy between parameters has to be removed by adding appropriate constraints to the global set (1).

The equations of motion result from the application of the Hamilton principle which can be written taking into account the system holonomic constraints (1) and the constraints which relate the material velocities and the time derivatives of generalized coordinates (3):

$$\delta \int_{t_1}^{t_2} \left\{ \frac{1}{2} \boldsymbol{v}^T \boldsymbol{M} \boldsymbol{v} - \boldsymbol{\mu}^T \left(\boldsymbol{v} - \boldsymbol{L}(\boldsymbol{q}) \dot{\boldsymbol{q}} \right) - \mathcal{V}(\boldsymbol{q}) - \boldsymbol{\lambda}^T \boldsymbol{\Phi}(\boldsymbol{q}) \right\} \mathrm{d}t = 0. \tag{4}$$

If we successively perform the variations of $\boldsymbol{\mu}$, $\boldsymbol{\lambda}$, $\boldsymbol{v}$ and $\boldsymbol{q}$:

- the variation of the multipliers $\boldsymbol{\mu}$ restores the velocity equations (3)
- the variation of the multipliers $\boldsymbol{\lambda}$ restores the constraints set (1)
- the variation $\delta \boldsymbol{v}$ shows that the multipliers $\boldsymbol{\mu}$ have the meaning of generalized momenta

$$\boldsymbol{\mu} = \boldsymbol{M} \boldsymbol{v}, \tag{5}$$

- the variation of the generalized displacements $\boldsymbol{q}$ yields

$$\int_{t_1}^{t_2} \left\{ \delta \boldsymbol{q}^T \left(-\frac{\partial \mathcal{V}}{\partial \boldsymbol{q}} - \frac{\partial \boldsymbol{\Phi}^T}{\partial \boldsymbol{q}} \boldsymbol{\lambda} + \frac{\partial}{\partial \boldsymbol{q}} [(\boldsymbol{L} \dot{\boldsymbol{q}})^T \boldsymbol{\mu}] \right) + \delta \dot{\boldsymbol{q}}^T \boldsymbol{L}^T \boldsymbol{\mu} \right\} \mathrm{d}t = 0, \tag{6}$$

  from which the equilibrium equations will be obtained.

The integration by parts of equation (6) yields

$$\left[\delta \boldsymbol{q}^T \boldsymbol{L}^T \boldsymbol{\mu} \right]_{t_1}^{t_2} + \int_{t_1}^{t_2} \delta \boldsymbol{q}^T \left\{ -\frac{\partial \mathcal{V}}{\partial \boldsymbol{q}} - \frac{\partial \boldsymbol{\Phi}^T}{\partial \boldsymbol{q}} \boldsymbol{\lambda} + \frac{\partial}{\partial \boldsymbol{q}} \left[(\boldsymbol{L} \dot{\boldsymbol{q}})^T \boldsymbol{\mu} \right] - \frac{\mathrm{d}}{\mathrm{d}t} \left(\boldsymbol{L}^T \boldsymbol{\mu} \right) \right\} \mathrm{d}t = 0 \tag{7}$$

and the combination of (5) and (3) yields

$$\boldsymbol{\mu} = \boldsymbol{M} \boldsymbol{L}(\boldsymbol{q}) \dot{\boldsymbol{q}}. \tag{8}$$

The equations of motion thus result in the form of a first-order differential-algebraic system of equations in $\boldsymbol{q}$, $\boldsymbol{\mu}$, and $\boldsymbol{\lambda}$:

$$\begin{cases} \boldsymbol{L}^T \dot{\boldsymbol{\mu}} + \dfrac{\partial \mathcal{V}}{\partial \boldsymbol{q}} + \boldsymbol{B}^T \boldsymbol{\lambda} + \dot{\boldsymbol{L}}^T \boldsymbol{\mu} - \dfrac{\partial}{\partial \boldsymbol{q}} [(\boldsymbol{L} \dot{\boldsymbol{q}})^T \boldsymbol{\mu}] = \boldsymbol{0}, \\ \boldsymbol{\mu} - \boldsymbol{M} \boldsymbol{L} \dot{\boldsymbol{q}} = \boldsymbol{0}, \\ \boldsymbol{\Phi} = \boldsymbol{0}, \end{cases} \tag{9}$$

where the matrix $\boldsymbol{B} = \partial\boldsymbol{\Phi}/\partial\boldsymbol{q}$ in Equation (9a) is the $R \times N$ Jacobian matrix of constraints. It is worth noting at this stage that the latter two terms in Equation (9a) can be put in the form

$$\dot{\boldsymbol{L}}^T\boldsymbol{\mu} - \frac{\partial}{\partial\boldsymbol{q}}[(\boldsymbol{L}\dot{\boldsymbol{q}})^T\boldsymbol{\mu}] = \boldsymbol{G}(\boldsymbol{\mu}, \boldsymbol{q})\dot{\boldsymbol{q}}, \tag{10}$$

where the skew-symmetric matrix $\boldsymbol{G}(\boldsymbol{\mu}, \boldsymbol{q})$ has the following components:

$$G_{jp} = \sum_i \mu_i \left(\frac{\partial L_{ij}}{\partial q_p} - \frac{\partial L_{ip}}{\partial q_j}\right). \tag{11}$$

The skew-symmetry of (11) follows from its very definition. The final form of the equations of motion is thus

$$\begin{cases} \boldsymbol{L}^T\dot{\boldsymbol{\mu}} + \dfrac{\partial \mathcal{V}}{\partial \boldsymbol{q}} + \boldsymbol{B}^T\boldsymbol{\lambda} + \boldsymbol{G}\dot{\boldsymbol{q}} = \boldsymbol{0}, \\ \boldsymbol{\mu} - \boldsymbol{M}\boldsymbol{L}\dot{\boldsymbol{q}} = \boldsymbol{0}, \\ \boldsymbol{\Phi} = \boldsymbol{0}. \end{cases} \tag{12}$$

3. Time Discretization Applying the Midpoint Rule

The mid-point integration rule is based on the application of the mean value theorem which states that, for any continuous and differentiable function $y(t)$, there is a scalar $\alpha \in [0, 1]$ such that $y(t + h)$ can be expressed in the form

$$y(t + h) = y(t) + h\left.\frac{\mathrm{d}y}{\mathrm{d}t}\right|_{t+\alpha h}. \tag{13}$$

When applied to the solution of a first-order nonlinear differential equation

$$\dot{\boldsymbol{y}} = \boldsymbol{f}(\boldsymbol{y}, t) \tag{14}$$

and imposing $\alpha = 1/2$, it yields the second-order accurate difference formula known as the mid-point rule

$$\boldsymbol{y}_{n+1} = \boldsymbol{y}_n + h\boldsymbol{f}(\boldsymbol{y}_{n+(1/2)}, t_{n+(1/2)}) + O(h^2) \quad \text{where} \quad t_{n+(1/2)} = \frac{1}{2}(t_n + t_{n+1}), \tag{15}$$

which is equivalent to the trapezoidal rule in the linear case. The application of the mid-point rule to the momenta and to the generalized coordinates time derivatives yields

$$\begin{aligned} \dot{\boldsymbol{\mu}}_{n+(1/2)} &= \frac{1}{h}(\boldsymbol{\mu}_{n+1} - \boldsymbol{\mu}_n), \\ \dot{\boldsymbol{q}}_{n+(1/2)} &= \frac{1}{h}(\boldsymbol{q}_{n+1} - \boldsymbol{q}_n). \end{aligned} \tag{16}$$

By making use of Equations (16) the equilibrium equation (12a) is thus discretized in the form

$$\frac{1}{h}\boldsymbol{L}_{n+(1/2)}^{T}(\boldsymbol{\mu}_{n+1}-\boldsymbol{\mu}_{n}) + \left(\frac{\partial \mathcal{V}}{\partial \boldsymbol{q}}+\boldsymbol{B}^{T}\boldsymbol{\lambda}\right)_{n+(1/2)} + \frac{1}{h}\boldsymbol{G}_{n+(1/2)}(\boldsymbol{q}_{n+1}-\boldsymbol{q}_{n}) = \boldsymbol{0}. \tag{17}$$

We also discretize the relationship (8) between momenta and time derivatives of the generalized coordinates expressed at the time $t_{n+(1/2)}$ in the form

$$\boldsymbol{\mu}_{n+(1/2)} = \frac{1}{2}(\boldsymbol{\mu}_{n+1}+\boldsymbol{\mu}_{n}) = \frac{1}{h}\boldsymbol{M}\boldsymbol{L}_{n+(1/2)}\,(\boldsymbol{q}_{n+1}-\boldsymbol{q}_{n}) \tag{18}$$

Combining (17) and (18) yields the final form of discretized equilibrium:

$$\frac{2}{h^{2}}\left(\boldsymbol{L}^{T}\boldsymbol{M}\boldsymbol{L}\right)_{n+(1/2)}(\boldsymbol{q}_{n+1}-\boldsymbol{q}_{n}) - \frac{2}{h}\boldsymbol{L}_{n+(1/2)}^{T}\boldsymbol{\mu}_{n} + \left(\frac{\partial \mathcal{V}}{\partial \boldsymbol{q}}+\boldsymbol{B}^{T}\boldsymbol{\lambda}\right)_{n+(1/2)} + \frac{1}{h}\boldsymbol{G}_{n+(1/2)}(\boldsymbol{q}_{n+1}-\boldsymbol{q}_{n}) = \boldsymbol{0}. \tag{19}$$

Equation (19) and the constraint equation (1) can both be solved in an iterative form to obtain $\boldsymbol{q}_{n+1}$ and $\boldsymbol{\lambda}_{n+(1/2)}$.

4. Energy Preservation in the Discrete Scheme

We study hereafter the properties of the integration scheme obtained in the previous section in order to achieve the preservation of the total energy. Let us multiply Equation (17) by the jump of displacements $\Delta\boldsymbol{q} = (\boldsymbol{q}_{n+1}-\boldsymbol{q}_{n})$ over the time step

$$\begin{aligned}&\frac{1}{h}(\boldsymbol{\mu}_{n+1}-\boldsymbol{\mu}_{n})^{T}\boldsymbol{L}_{n+(1/2)}(\boldsymbol{q}_{n+1}-\boldsymbol{q}_{n}) + (\boldsymbol{q}_{n+1}-\boldsymbol{q}_{n})^{T}\left(\frac{\partial \mathcal{V}}{\partial \boldsymbol{q}}\right)_{n+(1/2)} \\ &\quad + (\boldsymbol{q}_{n+1}-\boldsymbol{q}_{n})^{T}\left(\boldsymbol{B}^{T}\boldsymbol{\lambda}\right)_{n+(1/2)} + \frac{1}{h}(\boldsymbol{q}_{n+1}-\boldsymbol{q}_{n})^{T}\boldsymbol{G}_{n+(1/2)}(\boldsymbol{q}_{n+1}-\boldsymbol{q}_{n}) \\ &= I_1 + I_2 + I_3 + I_4 = 0.\end{aligned} \tag{20}$$

Expression (18) yields

$$\frac{1}{h}\boldsymbol{L}_{n+(1/2)}(\boldsymbol{q}_{n+1}-\boldsymbol{q}_{n}) = \boldsymbol{M}^{-1}\boldsymbol{\mu}_{n+(1/2)}. \tag{21}$$

By substituting (21) into the first term of Equation (20), we can see that it represents the jump of kinetic energy over the time step

$$\begin{aligned}I_1 &= (\boldsymbol{\mu}_{n+1}-\boldsymbol{\mu}_{n})^{T}\boldsymbol{M}^{-1}\boldsymbol{\mu}_{n+(1/2)} = (\boldsymbol{\mu}_{n+1}-\boldsymbol{\mu}_{n})^{T}\boldsymbol{M}^{-1}\frac{1}{2}(\boldsymbol{\mu}_{n}+\boldsymbol{\mu}_{n+1}) \\ &= \frac{1}{2}(\boldsymbol{\mu}_{n+1}^{T}\boldsymbol{M}^{-1}\boldsymbol{\mu}_{n+1} - \boldsymbol{\mu}_{n}^{T}\boldsymbol{M}^{-1}\boldsymbol{\mu}_{n}) = \mathcal{K}_{n+1} - \mathcal{K}_{n}.\end{aligned} \tag{22}$$

Note that the equality (22) does not depend of $\boldsymbol{L}_{n+(1/2)}$ i.e., of the parameterization of the rotations adopted.

We replace in the second term of Equation (20) the midpoint derivative $(\partial \mathcal{V}/\partial \boldsymbol{q})_{n+(1/2)}$ by the approximation $(\partial \mathcal{V}/\partial \boldsymbol{q})^*_{n+(1/2)}$ (*discrete directional derivative* [12]). This term represents the work produced by the potential forces over one time step and satisfies the following condition

$$I_2 = (\boldsymbol{q}_{n+1} - \boldsymbol{q}_n)^T \left. \frac{\partial \mathcal{V}}{\partial \boldsymbol{q}} \right|^*_{n+(1/2)} = \mathcal{V}_{n+1} - \mathcal{V}_n. \tag{23}$$

The third term in (20) can be put in the form

$$I_3 = (\boldsymbol{q}_{n+1} - \boldsymbol{q}_n)^T \left(\boldsymbol{B}^T \boldsymbol{\lambda}\right)_{n+(1/2)} = h \left(\boldsymbol{\lambda}^T \boldsymbol{B} \dot{\boldsymbol{q}}\right)_{n+(1/2)}. \tag{24}$$

It represents the work done by the constraints $\boldsymbol{\Phi}$ over the time step. To guarantee the preservation of the total energy of the system, this discrete work expression must vanish, i.e.

$$h \left(\boldsymbol{\lambda}^T \boldsymbol{B} \dot{\boldsymbol{q}}\right)_{n+(1/2)} = 0. \tag{25}$$

To achieve this, we make again use of the concept of *discrete directional derivative*, where the Jacobian matrix of constraints $\boldsymbol{B}_{n+(1/2)}$ is replaced by the approximation $\boldsymbol{B}^*_{n+(1/2)}$ such that

$$\boldsymbol{B}^*_{n+(1/2)}(\boldsymbol{q}_{n+1} - \boldsymbol{q}_n) = \boldsymbol{\Phi}_{n+1} - \boldsymbol{\Phi}_n. \tag{26}$$

With this condition

$$I_3 = (\boldsymbol{q}_{n+1} - \boldsymbol{q}_n)^T \left(\boldsymbol{B}^{*T} \boldsymbol{\lambda}\right)_{n+(1/2)} = (\boldsymbol{\Phi}_{n+1} - \boldsymbol{\Phi}_n)\boldsymbol{\lambda}_{n+(1/2)}. \tag{27}$$

The configuration at time t_n is assumed to be compatible, $\boldsymbol{\Phi}_n = \boldsymbol{0}$. Hence enforcing $\boldsymbol{\Phi}_{n+1} = \boldsymbol{0}$ the work done by the constraint forces vanishes, i.e.

$$I_3 = (\boldsymbol{q}_{n+1} - \boldsymbol{q}_n)^T \left(\boldsymbol{B}^{*T} \boldsymbol{\lambda}\right)_{n+(1/2)} = 0. \tag{28}$$

Finally the last term in (20) vanishes because of the skew-symmetric nature of the matrix $\boldsymbol{G}$ (Equation (11)):

$$I_4 = \frac{1}{h}(\boldsymbol{q}_{n+1} - \boldsymbol{q}_n)^T \boldsymbol{G}_{n+(1/2)}(\boldsymbol{q}_{n+1} - \boldsymbol{q}_n) = \frac{1}{h}\Delta \boldsymbol{q}^T \boldsymbol{G}_{n+(1/2)} \Delta \boldsymbol{q} = 0. \tag{29}$$

Satisfying all these conditions and replacing (22), (23), (28) and (29) into Equation (20) yields

$$\Delta \mathcal{K} + \Delta \mathcal{V} = 0. \tag{30}$$

It can thus be stated that the integration scheme formed by Equations (17) and (18) preserves the total energy of the system if

- the vanishing of the work done by the forces of constraints is guaranteed by means of the use of the *discrete directional derivative* matrix $\boldsymbol{B}^*_{n+(1/2)}$,
- the mid-point approximation of the internal and external forces is computed using the *discrete directional derivative* of the discrete forces from the potential $\mathcal{V}$ so that it guarantees the work done by the discrete forces equals the jump of potential energy,
- The skew-symmetric property of the $\boldsymbol{G}_{n+(1/2)}$ matrix is guaranteed.

5. Spherical Motion and Rotations Parameterization

Spherical motion corresponds to the rotation of a rigid body about a fixed point in space. The length of the position vector of a given point P attached to the body is not affected by the pure rotation and the relative angle between any two directions attached to the body remains constant under the transformation. If we describe with $\boldsymbol{X}$ the position vector of the point P in the reference configuration and with $\boldsymbol{x}$ the position vector of point P after transformation, the pure rotation can be expressed as the following linear transformation

$$\boldsymbol{x} = \boldsymbol{R}\boldsymbol{X}, \tag{31}$$

being $\boldsymbol{R}$ proper orthogonal

$$\boldsymbol{R}^T = \boldsymbol{R}^{-1} \quad \text{and} \quad \det(\boldsymbol{R}) = 1. \tag{32}$$

The absolute velocity vector of point P is computed as

$$\boldsymbol{v} = \dot{\boldsymbol{R}}\boldsymbol{X} = \boldsymbol{R}\widetilde{\boldsymbol{\Omega}}\boldsymbol{X}, \tag{33}$$

where $\widetilde{\boldsymbol{\Omega}}$ is the skew-symmetric matrix of angular velocities, defined by

$$\widetilde{\boldsymbol{\Omega}} = \boldsymbol{R}^T\dot{\boldsymbol{R}} = \begin{bmatrix} 0 & -\Omega_3 & \Omega_2 \\ \Omega_3 & 0 & -\Omega_1 \\ -\Omega_2 & \Omega_1 & 0 \end{bmatrix}. \tag{34}$$

The angular velocity vector can then be computed in terms of the rotation operator $\boldsymbol{R}$ as

$$\boldsymbol{\Omega} = \mathrm{vect}(\widetilde{\boldsymbol{\Omega}}) = \mathrm{vect}(\boldsymbol{R}^T\dot{\boldsymbol{R}}). \tag{35}$$

If we apply the midpoint rule to the time incrementation of the finite rotations, the discrete approximation of the angular velocities can be computed as

$$\widetilde{\boldsymbol{\Omega}}_{n+(1/2)} = \boldsymbol{R}^T_{n+(1/2)}\dot{\boldsymbol{R}}_{n+(1/2)} \simeq \frac{1}{h}\boldsymbol{R}^T_{n+(1/2)}(\boldsymbol{R}_{n+1} - \boldsymbol{R}_n). \tag{36}$$

In order to define the configuration that is half-way between $\boldsymbol{R}_n$ and $\boldsymbol{R}_{n+1}$ let us decompose the rotation increment from $\boldsymbol{R}_n$ to $\boldsymbol{R}_{n+1}$ in the form

$$\boldsymbol{R}^T_n\boldsymbol{R}_{n+1} = \boldsymbol{F}^2. \tag{37}$$

The resulting operator $\boldsymbol{F}$ is such that

$$\boldsymbol{R}_{n+(1/2)} = \boldsymbol{R}_n \boldsymbol{F} = \boldsymbol{R}_{n+1} \boldsymbol{F}^T \tag{38}$$

and verifies the properties of orthonormality

$$\boldsymbol{F}\boldsymbol{F}^T = \boldsymbol{F}^T \boldsymbol{F} = \boldsymbol{I}. \tag{39}$$

After replacing Equation (38) into (36), the angular velocity can be computed as

$$\widetilde{\boldsymbol{\Omega}}_{n+(1/2)} = \frac{1}{h}(\boldsymbol{F} - \boldsymbol{F}^T) \tag{40}$$

and the material rotational increment takes the form

$$\Delta\widetilde{\boldsymbol{\Theta}} = (\boldsymbol{F} - \boldsymbol{F}^T). \tag{41}$$

The operator $\boldsymbol{F}$ can be described in terms of the invariants $(\boldsymbol{n},\ \Delta\phi)$ of the relative rotation in the form

$$\boldsymbol{F} = \boldsymbol{R}\left(\boldsymbol{n}, \frac{1}{2}\Delta\phi\right). \tag{42}$$

If we choose for instance the Euler parameters, we have

$$\mathrm{vect}(\boldsymbol{F}) = \boldsymbol{n} \sin\frac{1}{2}\Delta\phi = \boldsymbol{e}, \tag{43}$$

where $\boldsymbol{e}$ is the vectorial part of the Euler parameters of the relative rotation. The operator $\boldsymbol{F}$ thus has the following explicit form

$$\boldsymbol{F} = e_0 \boldsymbol{I} + \frac{1}{1+e_0}\boldsymbol{e}\boldsymbol{e}^T + \widetilde{\boldsymbol{e}} \tag{44}$$

and we get the following simplified approximations

$$\boldsymbol{\Omega}_{n+(1/2)} \simeq \frac{2}{h}\boldsymbol{e}, \quad \Delta\boldsymbol{\Theta} \simeq 2\boldsymbol{e}. \tag{45}$$

After identification with Equation (3), we may see that for this parameterization the matrix $\boldsymbol{L}_{n+(1/2)} = 2\boldsymbol{I}$ is constant.

6. Analysis of the Most Usual Constraints

Joints are a distinguishing feature of multibody systems that impose constraints on the relative motion between system bodies. In this work, the forces associated to constraints are discretized in such a way that the work they perform exactly vanishes at each time step. The most usual joints can be modelled in terms of the so-called *lower pairs* (Figure 1): the revolute, prismatic, screw, cylindrical, planar and spherical joints [8, 11]. These kinematic pairs can be expressed as a linear combination of some of the following constraint equations:

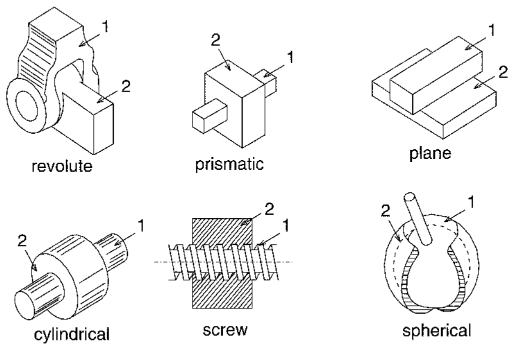

Figure 1. Most usual joints in multibody systems.

(a) $\Phi = (1/2)\boldsymbol{q}^T \boldsymbol{C}_2 \boldsymbol{q} + \boldsymbol{c}_1^T q + c_0,$
(b) $\Phi = \boldsymbol{u}^T \boldsymbol{R} \boldsymbol{v},$
(c) $\Phi = \cos\alpha(\boldsymbol{u}\cdot\boldsymbol{w}) - \sin\alpha(\boldsymbol{v}\cdot\boldsymbol{w}),$

where $\boldsymbol{q}$ is a coordinate vector, $\boldsymbol{C}_2$ is a symmetric matrix with constant coefficients, $\boldsymbol{c}_1$, $\boldsymbol{u}$, $\boldsymbol{v}$ and $\boldsymbol{w}$ are constant vectors and c_0 is a constant. Next, the work done by each of these constraints over a time step will be studied and the corresponding $\boldsymbol{B}^*_{n+(1/2)}$ matrix expression will be done in each case. For the first constraint equation we have:

$$\begin{aligned}\boldsymbol{B}_{n+(1/2)}\Delta\boldsymbol{q} &= \left.\frac{\partial\boldsymbol{\Phi}}{\partial\boldsymbol{q}}\right|_{n+(1/2)}(\boldsymbol{q}_{n+1}-\boldsymbol{q}_n)\\ &= \left[\frac{1}{2}(\boldsymbol{q}_{n+1}+\boldsymbol{q}_n)^T\boldsymbol{C}_2+\boldsymbol{c}_1\right](\boldsymbol{q}_{n+1}-\boldsymbol{q}_n)\\ &= \frac{1}{2}(\boldsymbol{q}_{n+1}^T\boldsymbol{C}_2\boldsymbol{q}_{n+1}-\boldsymbol{q}_n^T\boldsymbol{C}_2\boldsymbol{q}_n)+\boldsymbol{c}_1(\boldsymbol{q}_{n+1}-\boldsymbol{q}_n)\\ &= \boldsymbol{\Phi}_{n+1}-\boldsymbol{\Phi}_n. \end{aligned} \tag{46}$$

Then we see that for this case, we have

$$\boldsymbol{B}^*_{n+(1/2)} = \boldsymbol{B}_{n+(1/2)}. \tag{47}$$

For (b), we can see that

$$\begin{aligned}\left.\frac{\partial\Phi}{\partial\boldsymbol{\Theta}}\right|^*_{n+(1/2)}\Delta\boldsymbol{\Theta} &= \boldsymbol{u}^T\boldsymbol{R}_{n+(1/2)}\Delta\widetilde{\boldsymbol{\Theta}}\boldsymbol{v} = \boldsymbol{u}^T\boldsymbol{R}_{n+(1/2)}(\boldsymbol{F}-\boldsymbol{F}^T)\boldsymbol{v}\\ &= \boldsymbol{u}^T\boldsymbol{R}_{n+(1/2)}\boldsymbol{F}\boldsymbol{v}-\boldsymbol{u}^T\boldsymbol{R}_{n+(1/2)}\boldsymbol{F}^T\boldsymbol{v} = \boldsymbol{\Phi}_{n+1}-\boldsymbol{\Phi}_n, \end{aligned} \tag{48}$$

where $\Delta\boldsymbol{\Theta} = \boldsymbol{L}_{n+(1/2)}\Delta\boldsymbol{q}$.

Therefore, the discrete directional derivative of the constraints results

$$\boldsymbol{B}^*_{n+(1/2)} = -\boldsymbol{u}^T\boldsymbol{R}_{n+(1/2)}\tilde{\boldsymbol{v}}\boldsymbol{L}_{n+(1/2)}. \tag{49}$$

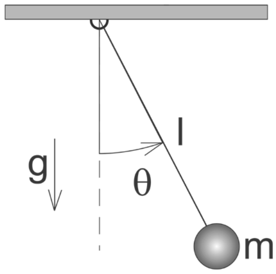

Figure 2. Simple pendulum.

We can rewrite equation (c) as a linear combination of functions of the following type

$$\Phi = g(\alpha)(\boldsymbol{v} \cdot \boldsymbol{u}) = 0, \tag{50}$$

where $g(\alpha)$ is $\sin\alpha$ or $\cos\alpha$. Then we have

$$\begin{aligned} B^*_{n+(1/2)}\Delta q &= \left.\frac{\partial \Phi}{\partial \alpha}\right|^*_{n+(1/2)} \Delta\alpha = (\boldsymbol{u}\cdot\boldsymbol{v})g^{*\prime}(\alpha_{n+1}-\alpha_n) \\ &= B^*_{n+(1/2)}(\alpha_{n+1}-\alpha_n) = \Phi_{n+1} - \Phi_n, \end{aligned} \tag{51}$$

where the discrete derivative $g^{*\prime}$ is computed from the following expression:

$$(g_{n+1} - g_n) = g^{*\prime}(\alpha_{n+1} - \alpha_n). \tag{52}$$

For example, if $g(\alpha) = \sin\alpha$, we have

$$\begin{aligned} \sin\alpha_{n+1} - \sin\alpha_n &= \frac{\sin\frac{\alpha_{n+1}-\alpha_n}{2}}{\frac{\alpha_{n+1}-\alpha_n}{2}} \cos\frac{\alpha_{n+1}+\alpha_n}{2}(\alpha_{n+1}-\alpha_n) \\ &= g^{*\prime}(\alpha_{n+1}-\alpha_n), \end{aligned} \tag{53}$$

where we identify

$$B^*_{n+(1/2)} = (\boldsymbol{u}\cdot\boldsymbol{v})\frac{\sin\frac{\alpha_{n+1}-\alpha_n}{2}}{\frac{\alpha_{n+1}-\alpha_n}{2}} \cos\frac{\alpha_{n+1}+\alpha_n}{2}. \tag{54}$$

We proceed in a similar way for $g(\alpha) = \cos\alpha$.

Therefore, we can see that the following constraint equation

$$\Phi = c_0 + \boldsymbol{c}_1\boldsymbol{q} + \boldsymbol{q}^T\boldsymbol{C}_2\boldsymbol{q} + c_3\boldsymbol{u}^T\boldsymbol{R}\boldsymbol{v} + c_4\boldsymbol{u}^T\cos\alpha\boldsymbol{v} + c_5\boldsymbol{u}^T\sin\alpha\boldsymbol{v} \tag{55}$$

can be formulated in an energy preserving time integration scheme.

7. Numerical Applications

7.1. SIMPLE PENDULUM

The first example deals with the simple pendulum depicted in Figure 2. The system has one degree of freedom $q = \theta$. The corresponding kinetic and potential energy expressions are:

$$\begin{aligned} \mathcal{K} &= \frac{1}{2} m \dot{\theta}^2 \ell^2, \\ \mathcal{V} &= (1 - \cos\theta) m g \ell. \end{aligned} \tag{56}$$

By making use of very simple trigonometric relationships we express the potential energy in terms of $\theta/2$ instead of θ.

$$(1 - \cos\theta) m g \ell = 2 \sin^2 \frac{\theta}{2} m g \ell. \tag{57}$$

The particle has a mass m, the pendulum length is ℓ and the matrices $\boldsymbol{L}$ and $\boldsymbol{G}$ are $\boldsymbol{I}$ and $\boldsymbol{0}$ respectively. The infinitesimal displacements and the linear momenta expressions are

$$\delta w = \delta q = \delta\theta, \quad \mu = p = m v = m \ell \dot{\theta}. \tag{58}$$

Hence the discrete equations of motions are

$$\frac{2}{h^2} m \ell \left(\theta_{n+1} - \theta_n\right) - \frac{2}{h} m \ell \dot{\theta}_n + \left.\frac{\partial \mathcal{V}}{\partial \theta}\right|^{*}_{n+(1/2)} = 0, \tag{59}$$

where the external forces at the mid-point must satisfy the relationship (23). Finally the discrete equation for the energy preserving scheme results

$$\begin{aligned} &\frac{2}{h^2} m \ell \left(\theta_{n+1} - \theta_n\right) - \frac{2}{h} m \ell \dot{\theta}_n \\ &\quad + \frac{2 m g \ell}{\theta_{n+1} - \theta_n} \left(\left.\sin^2 \frac{\theta}{2}\right|_{n+1} - \left.\sin^2 \frac{\theta}{2}\right|_{n} \right) = 0. \end{aligned} \tag{60}$$

The resulting scheme accordingly modified, is identical with Greenspan's energy conserving method [13].

Note that if we evaluate the external forces exactly at the mid-point instead of evaluating the approximation of the discrete external forces from Equation (60), the following scheme results

$$\frac{2}{h^2} m \ell \left(\theta_{n+1} - \theta_n\right) - \frac{2}{h} m \ell \dot{\theta}_n + m g \ell \left(\sin \frac{\theta_{n+1} + \theta_n}{2} \right) = 0. \tag{61}$$

This is the trapezoidal rule from the Newmark family of algorithms which is unconditional stable only in the linear regime. In Figure 3 the time evolution for the total energy of the system for both schemes is plotted. It can be seen that the trapezoidal rule does not preserve the total energy of the system.

Figure 4 shows that the preserving scheme verifies second-order accuracy for this example.

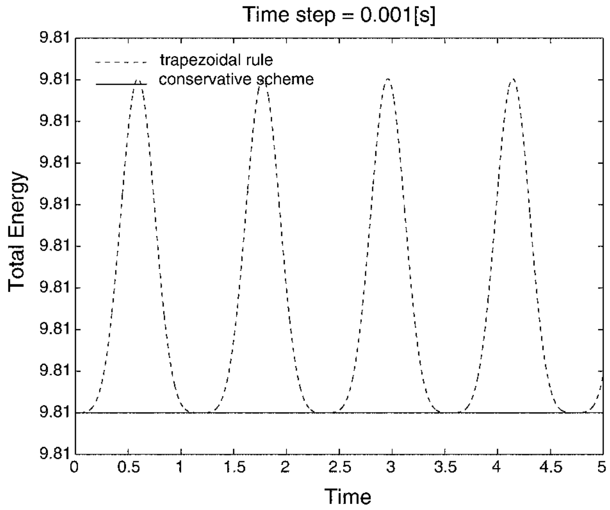

Figure 3. Simple pendulum: time history of the total energy for the trapezoidal rule and for the energy preserving scheme.

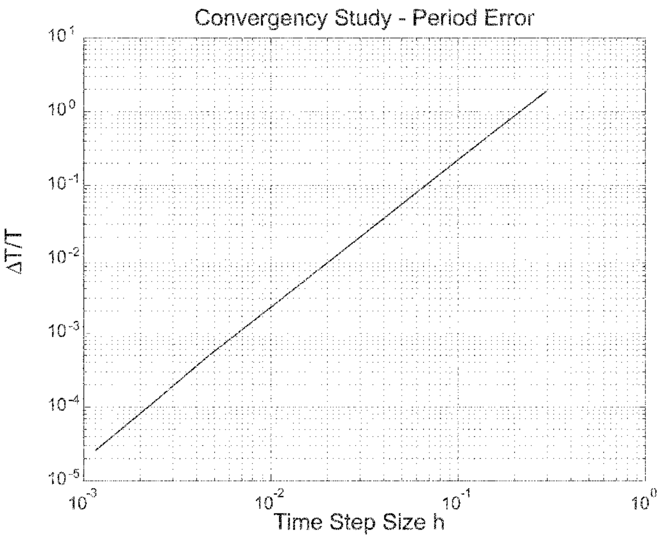

Figure 4. Simple Pendulum: Convergence study.

7.2. DOUBLE PENDULUM

The second example deals with the double pendulum depicted in Figure 5. In this case the system is considered as a general rigid multibody system with four degrees of freedom subject to two kinematic constraints. The system degrees of freedom are

$$\boldsymbol{q}^T = \left[\, x_1 \;\; y_1 \;\; x_2 \;\; y_2 \,\right]. \tag{62}$$

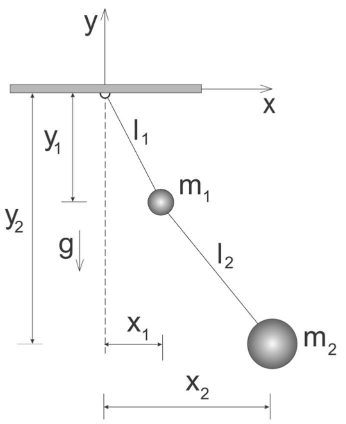

Figure 5. Double pendulum.

The kinetic and potential energies have the form

$$\begin{aligned} \mathcal{K} &= \frac{1}{2}m_1(\dot{x}_1^2 + \dot{y}_1^2) + \frac{1}{2}m_2(\dot{x}_2^2 + \dot{y}_2^2), \\ \mathcal{V} &= m_1 g y_1 + m_2 g y_2. \end{aligned} \tag{63}$$

The kinematic constraints are

$$\boldsymbol{\Phi} = \begin{bmatrix} x_1^2 + y_1^2 - \ell_1^2 \\ (x_2 - x_1)^2 + (y_2 - y_1)^2 - \ell_2 \end{bmatrix}. \tag{64}$$

The mass matrix and the velocities vector:

$$\boldsymbol{M} = \operatorname{diag}\begin{bmatrix} m_1 & m_1 & m_2 & m_2 \end{bmatrix}, \quad \boldsymbol{v} = \dot{\boldsymbol{q}}. \tag{65}$$

In this example the matrix $\boldsymbol{L}$ is the identity matrix and the matrix $\boldsymbol{G}$ is zero. The infinitesimal displacements and linear momentum vectors are written as

$$\delta\boldsymbol{w} = \delta\boldsymbol{x} = \delta\boldsymbol{q}, \quad \boldsymbol{\mu} = \boldsymbol{p} = \boldsymbol{M}\boldsymbol{v}. \tag{66}$$

The potential energy in (63) generates the external forces vector

$$\boldsymbol{g}_{\text{ext}}^T = \begin{bmatrix} 0 & -m_1 g & 0 & -m_2 g \end{bmatrix} \tag{67}$$

and the Jacobian matrix of constraints is

$$\boldsymbol{B} = \begin{bmatrix} 2x_1 & 2x_2 & 0 & 0 \\ 2(x_1 - x_2) & 2(y_1 - y_2) & 2(x_2 - x_1) & 2(y_2 - y_1) \end{bmatrix}. \tag{68}$$

Replacing in (19), the discrete equations of motion finally result

$$\begin{cases} \dfrac{2}{h^2}\boldsymbol{M}(\boldsymbol{x}_{n+1} - \boldsymbol{x}_n) - \dfrac{2}{h}\boldsymbol{M}\boldsymbol{v}_n + \boldsymbol{g}_{\text{ext}} + \boldsymbol{B}_{n+(1/2)}^T\boldsymbol{\lambda}_{n+(1/2)} = \boldsymbol{0}, \\ x{1}_{n+1}^2 + y{1}_{n+1}^2 - \ell_1^2 = 0, \\ (x_{2n+1} - x_{1n+1})^2 + (y_{2n+1} - y_{1n+1})^2 - \ell_2^2 = 0. \end{cases} \tag{69}$$

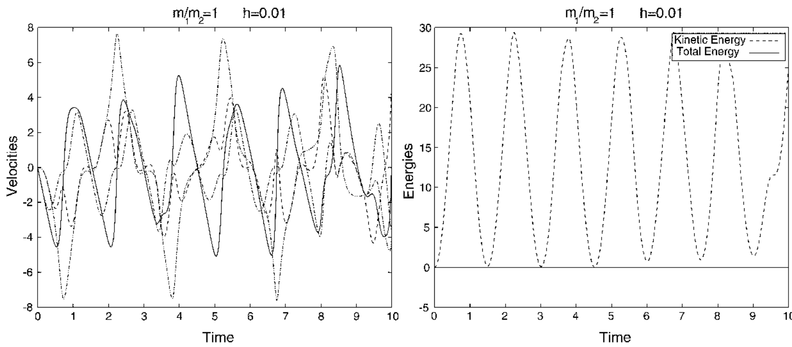

Figure 6. Double pendulum: Velocities and energies time histories for $m_1 = m_2 = 1$ and $h = 0.01$.

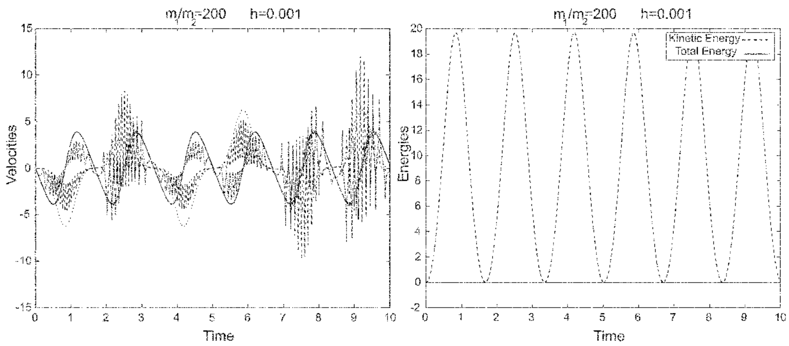

Figure 7. Double pendulum: Velocities and energies time histories for $m_1 = 0.005$, $m_2 = 1$ and $h = 0.001$.

The chosen values for the different parameters are $l_1 = 1$, $l_2 = 1$ and $g = 9.81$. The initial conditions are

$$\boldsymbol{x}_0^T = \begin{bmatrix} 1 & 0 & 1 & 1 \end{bmatrix} \quad \text{and} \quad \boldsymbol{v}_0^T = \begin{bmatrix} 0 & 0 & 0 & 0 \end{bmatrix}. \tag{70}$$

Figure 6 shows the velocity and energies time histories for a system with equal masses and a time step size $h = 0.01$. Figure 7 displays the velocity and energies time histories for $m_1 = 0.005$, $m_2 = 1$ (giving rise to a nearly singular mass matrix) and a time step size of $h = 0.001$. We can observe the growing oscillations in the velocities response due to the ill-conditioning of the mass matrix $\boldsymbol{M}$. Nevertheless, the total energy of the system is well preserved. For a time step size of $h = 0.01$ the solution diverges. On this example, the HHT scheme did not converge for either time step size.

7.3. SYMMETRICAL TOP IN GRAVITATIONAL FIELD

The top is modelled as a general rigid body (six generalized degrees of freedom) and is subject to three kinematic constraints. Let us adopt the centre of the mass of

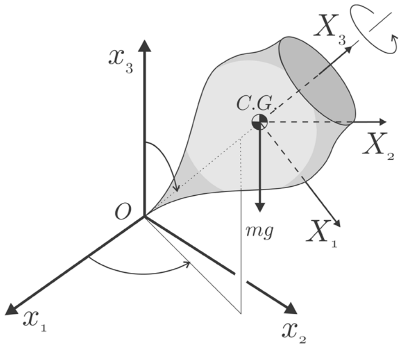

Figure 8. Symmetrical top.

the top as the origin of the material frame and its attachment point as the origin of the spatial frame. The top kinetic energy may be written as

$$\mathcal{K} = \frac{1}{2}\left(\boldsymbol{\Omega}^T \boldsymbol{J}\boldsymbol{\Omega} + m\dot{\boldsymbol{x}}^T\dot{\boldsymbol{x}}\right). \tag{71}$$

Assuming that the reference for the potential energy is the origin of the spatial frame, the potential energy may be expressed in the form

$$\mathcal{V} = -m\boldsymbol{g}^T\boldsymbol{x}, \tag{72}$$

where $\boldsymbol{g}$ is the acceleration vector. For example, if the gravity is acting along the axis x_3, $\boldsymbol{g} = [0 \quad 0 - g]^T$ and $\mathcal{V} = +mgx_3$. Finally, let us denote by $-\boldsymbol{X}_g$ the location of the top attachment point in material coordinates. The center of the mass is then constrained to verify at any time t the geometric relationship

$$\boldsymbol{\Phi} = -\boldsymbol{x} + \boldsymbol{R}\boldsymbol{X}_g = \boldsymbol{0}. \tag{73}$$

The mass matrix and the velocities vector are

$$\boldsymbol{M} = \begin{bmatrix} m\boldsymbol{I} & \boldsymbol{0} \\ \boldsymbol{0} & \boldsymbol{J} \end{bmatrix}, \quad \boldsymbol{v} = \begin{bmatrix} \dot{\boldsymbol{x}} \\ \boldsymbol{\Omega} \end{bmatrix} = \boldsymbol{L}\dot{\boldsymbol{q}}. \tag{74}$$

The specific choice of the rotation parameters will be done later. The translational and rotational infinitesimal displacements vector is written as

$$\delta\boldsymbol{w} = \begin{bmatrix} \delta\boldsymbol{x} \\ \delta\boldsymbol{\Theta} \end{bmatrix} = \begin{bmatrix} \boldsymbol{I} & \boldsymbol{0} \\ \boldsymbol{0} & \boldsymbol{T}(\boldsymbol{\Psi}) \end{bmatrix} \begin{bmatrix} \delta\boldsymbol{x} \\ \delta\boldsymbol{\Psi} \end{bmatrix} = \boldsymbol{L}\delta\boldsymbol{q}. \tag{75}$$

The generalized momentum vector is split into linear and angular momenta

$$\boldsymbol{\mu} = \begin{bmatrix} \boldsymbol{p} \\ \boldsymbol{h} \end{bmatrix}. \tag{76}$$

The potential energy (72) due to the gravity depends only of the translation motion and generates a constant external forces vector

$$-\frac{\partial\mathcal{V}}{\partial\boldsymbol{q}} = \begin{bmatrix} m\boldsymbol{g} \\ \boldsymbol{0} \end{bmatrix}. \tag{77}$$

The variation of kinematic constraints yields

$$\delta\boldsymbol{\Phi} = -\delta\boldsymbol{x} + \delta\boldsymbol{R}\boldsymbol{X}_g = -\begin{bmatrix} \boldsymbol{I} & \boldsymbol{R}\widetilde{\boldsymbol{X}}_g \end{bmatrix}\delta\boldsymbol{w} = \boldsymbol{B}\delta\boldsymbol{q} \tag{78}$$

with the Jacobian matrix of constraints

$$\boldsymbol{B} = \begin{bmatrix} -\boldsymbol{I} \\ \widetilde{\boldsymbol{X}}_g\boldsymbol{R}^T \end{bmatrix}^T \boldsymbol{L}. \tag{79}$$

Finally, the matrix $\boldsymbol{G}$ contributes only to the rotation motion. Taking into account the specific properties of the tangent operator of finite rotations it can be written as

$$\boldsymbol{G}(\boldsymbol{\mu}) = \boldsymbol{L}^T \begin{bmatrix} \boldsymbol{0} & \boldsymbol{0} \\ \boldsymbol{0} & -\widetilde{\boldsymbol{h}} \end{bmatrix} \boldsymbol{L}. \tag{80}$$

In terms of Euler parameters, the operator $\boldsymbol{F}$ can be written as (44) and with the approximations done in (45), the jump of the rotation parameters over a time step is

$$\Delta\boldsymbol{q} = \boldsymbol{q}_{n+1} - \boldsymbol{q}_n = \begin{bmatrix} \boldsymbol{x}_{n+1} - \boldsymbol{x}_n \\ 2\boldsymbol{e} \end{bmatrix} \tag{81}$$

and the tangent operator $\boldsymbol{L}$ in the mid-point is expressed as

$$\boldsymbol{L}_{n+(1/2)} = \begin{bmatrix} \boldsymbol{I} & \boldsymbol{0} \\ \boldsymbol{0} & 2\boldsymbol{I} \end{bmatrix} \tag{82}$$

The Jacobian matrix of constraints is computed as

$$\boldsymbol{B}^T_{n+(1/2)} = \begin{bmatrix} -\boldsymbol{I} \\ 2\widetilde{\boldsymbol{X}}_g\boldsymbol{R}^T_{n+(1/2)} \end{bmatrix}. \tag{83}$$

Finally, according to (80) the matrix $\boldsymbol{G}$ contributes only to the rotation motion in the form

$$\boldsymbol{G}_{n+(1/2)} = -\begin{bmatrix} \boldsymbol{0} & \boldsymbol{0} \\ \boldsymbol{0} & 4\widetilde{\boldsymbol{h}}_{n+(1/2)} \end{bmatrix}. \tag{84}$$

Particularizing the equilibrium equations (19) to the top motion and separating the translation and rotation parts of the motion yields the following set of discrete equations

$$\begin{cases} \dfrac{2}{h^2}m(\boldsymbol{x}_{n+1} - \boldsymbol{x}_n) - \dfrac{2}{h}m\boldsymbol{v}_n - \boldsymbol{\lambda}_{n+(1/2)} = m\boldsymbol{g}, \\ \dfrac{8}{h^2}\boldsymbol{J}\boldsymbol{e} - \dfrac{4}{h}\boldsymbol{J}\boldsymbol{\Omega}_n + \dfrac{8}{h^2}\widetilde{\boldsymbol{e}}\boldsymbol{J}\boldsymbol{e} + 2\widetilde{\boldsymbol{X}}_g\boldsymbol{R}^T_{n+(1/2)}\boldsymbol{\lambda}_{n+(1/2)} = \boldsymbol{0}, \\ -\boldsymbol{x}_{n+1} + \boldsymbol{R}_{n+1}\boldsymbol{X}_g = \boldsymbol{0}. \end{cases} \tag{85}$$

The evaluation of the corresponding iteration matrix is straightforward.

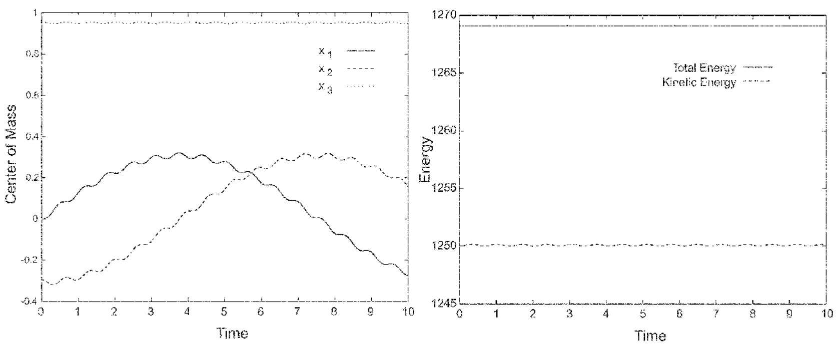

Figure 9. Symmetrical top: Position of the center of mass and kinetic and total energies.

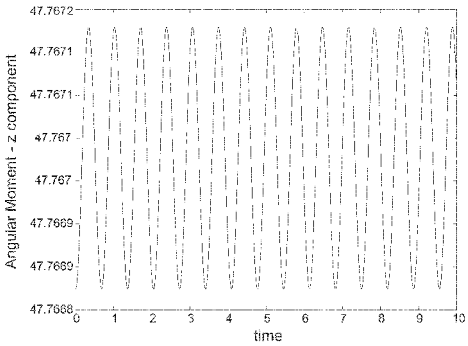

Figure 10. Symmetrical top: z component of the angular moment.

Let us take a symmetrical top with the following properties: $J_{11} = 5$, $J_{22} = 5$ and $J_{33} = 1$ its inertia tensor measured from the fixation point, $L = 1$ the distance from the center of mass to the fixation point, $g = 9.81$ the gravity acceleration acting along the x_3 axis and a mass m such as $mgL = 20$. The initial conditions in terms of Euler angles are $\phi_0 = 0$, $\theta_0 = 0.3$, $\psi_0 = 0$. The top is simply dropped from its initial position with a spin velocity of 50 rad/s.

Figure 9 shows the computed responses for a fixed time step size of $h = 0.001$ presented in various forms, namely the position of the center of the mass and total and kinetic energies. The total energy of the system is preserved as it was expected, because of the algorithm design. All time evolutions show that the periodical character is perfectly conserved, which can be seen as a direct consequence of the energy preservation. The results match with those obtained by Simo et al. [16]. Even if the conservation of the angular momentum component which lies parallel to the gravitational field is not algorithmically guaranteed, it is almost conserved with small oscillations as shown in Figure 10.

7.4. IMPACT BETWEEN RIGID BODIES

When two rigid bodies undergo contact, the contact condition is an inequality $q \geq 0$ which can be transformed into an equality condition $q - r^2 = 0$ through the addition of a slack variable r. Hence, the contact condition is enforced as a nonlinear holonomic constraint

$$\Phi = q - r^2 = 0. \tag{86}$$

The constraint forces arise from

$$\delta\Phi\lambda = \begin{bmatrix} \delta q \\ \delta r \end{bmatrix}^T \begin{bmatrix} \lambda \\ -2\lambda r \end{bmatrix} \tag{87}$$

and are discretized in such a way that the work they perform vanishes over a time step. The discrete forces are expressed as

$$\begin{bmatrix} \lambda_{n+(1/2)} \\ -2\lambda_{n+(1/2)} r_{n+(1/2)} \end{bmatrix}, \tag{88}$$

where $r_{n+(1/2)} = (r_{n+1} + r_n)/2$. The work done by the discretized forces of constraint is computed as $(\Phi_{n+1} - \Phi_n)\lambda_{n+(1/2)}$. In a similar manner as it was done in Section 4, by enforcing $\Phi_{n+1} = 0$ the vanishment of the discrete work and the avoidance of the drift phenomenon are guaranteed.

Since the slack variable is not connected to any degree of freedom of the model, the variation δr gives rise to the non linear equation $-2\lambda_{n+(1/2)} r_{n+(1/2)} = 0$ which possesses two solutions. The first one, $\lambda_{n+(1/2)} = 0$ is asociated to the non contact condition. The second one, $r_{n+(1/2)} = 0$ indicates an active contact condition and implies $r_{n+1} = -r_n$, which together with $\Phi_{n+1} = \Phi_n = 0$ results in $q_{n+1} = r_{n+1}^2 = r_n^2 = q_n$. In other words, when the contact condition is activated, a contact force $\lambda_{n+(1/2)} \neq 0$ is developed and the relative distance between the contacting bodies remains unchanged. We use for this example the relationship between velocities and displacements given by Equation (18):

$$\frac{\dot{q}_{n+1} + \dot{q}_n}{2} = \frac{q_{n+1} - q_n}{h}, \tag{89}$$

which yields $\dot{q}_{n+1} = \dot{q}_n$. For further details, see [2]. Laursen and Love [14] also deal with implicit integrators for transient impact problems introducing the idea of a *discrete contact velocity*.

Figure 11 shows the impact between two pendulums of unit mass and length. The problem has four degrees of freedom $\boldsymbol{q}^T = [x_1 \quad x_2 \quad y_1 \quad y_2]$, and is subjected to two length constraints $\Phi_1 = x_1^2 + y_1^2 - \ell_1^2 = 0$ and $\Phi_2 = x_2^2 + y_2^2 - \ell_2^2 = 0$, and the intermittent contact constraint. The right pendulum is dropped from its horizontal position with initial velocity $v_0 = 0$.

Figure 12 displays the time history of displacements and velocities for both bodies, where it can be seen once again that the periodic character is perfectly

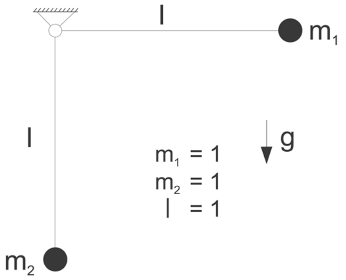

Figure 11. Two pendulums with mutual impact.

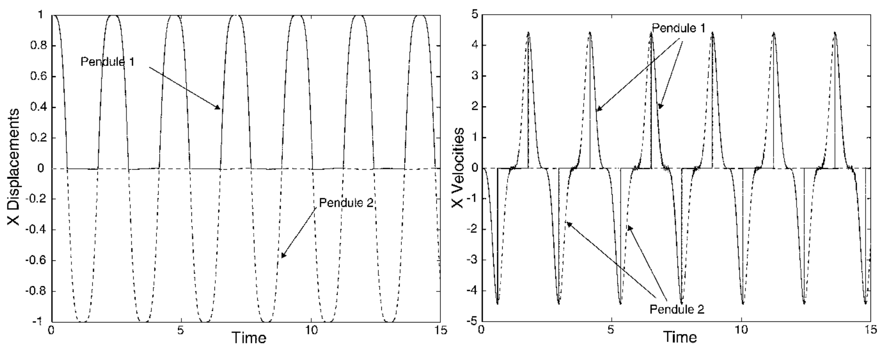

Figure 12. Displacements and velocities vs. time – x coordinate.

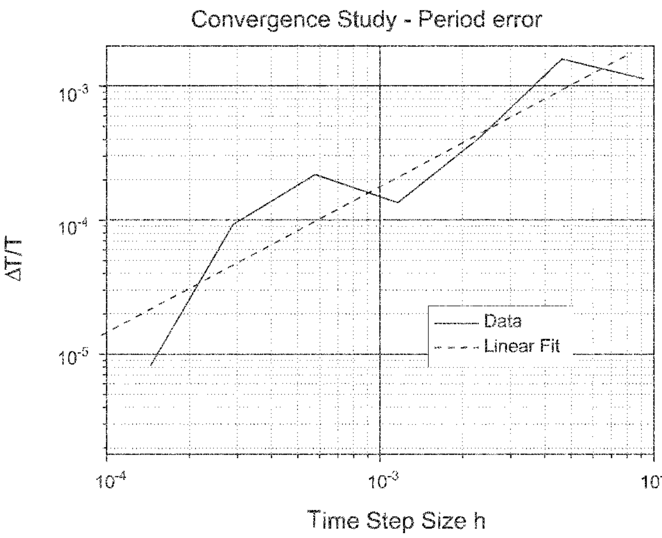

Figure 13. Two pendulums mutual impact: Convergence study.

preserved. Once again, this example could not be solved using the HHT scheme. Figure 13 shows that for this example the scheme verifies first order accuracy.

8. Conclusions

Integration methods which guarantee energy preservation represent an effective solution for time integration for the second order algebraic-differential equations since they provide a natural way to avoid the instability due to the non linearity of the system and the kinematic constraints.

We want to point out that in flexible problems or in rigid problems with mass ill conditioning, the numerical solution can develop spurious high frequency oscillations. These oscillations are preserved by the algorithm and can lead to the damage of the computation. Therefore the introduction of numerical dissipation in this frequency range is desired in order to annihilate the unwanted oscillations which can compromise the convergence of the solution.

Other interesting aspects to study are the implementation of the automatic control of the time step size, the treatment of non holonomic constraints and the consideration of more general integration rules which include as a particular case the mid point rule. These aspects will be the object of future work.

References

1. Bauchau, O., 'Computational schemes for flexible, nonlinear multi-body systems', *Multibody System Dynam.* **2**, 1998, 169–225.
2. Bauchau, O., 'Flexible multibody systems with intermittent contacts', *Multibody System Dynam.* **4**, 2000, 23–54.
3. Bauchau, O. and Joo, T., 'Computational schemes for nonlinear elasto-dynamics, *Internat. J. Numer. Meth. Engrg.* **45**, 1999, 693–719.
4. Betsch, P. and Steinmann, P., 'Conservation properties of a time FE method. Part I: Time-stepping schemes for N-body problems', *Internat. J. Numer. Meth. Engrg.* **49**, 2000, 599–638.
5. Betsch, P. and Steinmann, P., 'Conservation properties of a time FE method. Part II: Time-stepping schemes for non-linear elastodynamics', *Internat. J. Numer. Meth. Engrg.* **50**, 2001, 1931–1955.
6. Betsch, P. and Steinmann, P., 'Conservation properties of a time FE method. Part III: Mechanical systems with holonomic constraints, *Internat. J. Numer. Meth. Engrg.*, to appear.
7. Betsch, P. and Steinmann, P., 'Constrained integration of rigid body dynamics', *Comput. Methods Appl. Mech. Engrg.* **191**, 2001, 467–488.
8. Cardona, A., 'An integrated approach to mechanism analysis', Ph.D. Thesis, Faculté des Sciences Appliquées, Université of Liège, 1989.
9. Cardona, A. and Géradin, M., 'Time integration of the equations of motion in mechanism analysis, *Comput. & Structures Multibody* **33**, 1989, 801–820.
10. Chung, J. and Hulbert, G.M., 'A time integration algorithm for structural dynamics with improved numerical dissipation: The generalized α method', *J. Appl. Mech.* **60**, 1993, 371–375.
11. Géradin, M. and Cardona, A., *Flexible Multibody Dynamics: A Finite Element Approach*, John Wiley & Sons, New York, 2000.
12. Gonzalez, O., 'Mechanical systems subject to holonomic constraints: Differential-algebraic formulations and conservative integration', *Physica D* **132**, 1999, 165–174.

13. Greenspan, D., 'Conservative numerical methods for $\ddot{x} = f(x)$', *J. Comput. Phys.* **56**, 1984, 28–41.
14. Laursen, T.A. and Love, G.R., 'Improved implicit integrators for transient impact problems – Geometric admissibility within the conserving framework, *Internat. J. Numer. Meth. Engrg.* **53**, 2002, 245–274.
15. Puso, M., 'An energy and momentum conserving method for rigid-flexible body dynamics', *Internat. J. Numer. Meth. Engrg.* **53**, 2002, 1393–1414.
16. Simo, J.C., Tarnow, N. and Wong, K.K., 'Exact energy-momentum conserving algorithms and symplectic schemes for nonlinear dynamics', *Comput. Methods Appl. Mech. Engrg.* **100**, 1992, 63–116.
17. Whittaker, E.T., *Treatise on the Analytical Dynamics of Particles and Rigid Bodies*, fourth edition, Cambridge University Press, Cambridge, 1998.